N89-15952

ATTITUDE ANALYSIS OF THE EARTH RADIATION BUDGET SATELLITE (ERBS) YAW TURN ANOMALY

J. Kronenwetter and M. Phenneger, Computer Sciences Corporation (CSC)

W. Weaver, National Aeronautics and Space Administration/Langley Research Center (NASA/LRC)

ABSTRACT

The July 2 Earth Radiation Budget Satellite (ERBS) hydrazine thruster-controlled yaw inversion maneuver resulted in a 2.1 degree per second (deg/sec) attitude spin. This mode continued for 150 minutes (min) until the spacecraft was inertially despun using the hydrazine thrusters. The spacecraft remained in a low-rate Y-axis spin of .06 deg/sec for 3 hours until the B-DOT control mode was activated. After 5 hours in this mode, the spacecraft Y-axis was aligned to the orbit normal, and the spacecraft was commanded to the mission mode of attitude control.

This work presents the experience of real-time attitude determination support following analysis using the playback telemetry tape recorded for 7 hours from the start of the attitude control anomaly. For the high-spin-rate mode, sunlit portions of the orbit, the Sun data are used with dynamic interpolation of the gaps to derive the path of the Sun through the light-sensitive science instrument sensor and solar array fields of view. During the despun mode, results from ERBS Attitude Determination System (ADS) processing of the magnetometer data show graphically the alignment and slow rotation of the body coordinate system in the geocentric inertial (GCI) reference frame. These data provide an evaluation and explanation of the marginal power condition during the despun recovery period. Comparisons of the attitude results with science sensor output are provided to illustrate the impact of the attitude control anomaly on the science instruments. The paper concludes with an assessment of the experience gained and suggestions for additional procedures and software to provide spacecraft attitude maneuver and contingency support.

1. INTRODUCTION

On July 2, 1987, a thruster actuated, yaw inversion test maneuver with a disabled X-axis inertial reference unit (IRU) resulted in an uncontrolled tumble of the Earth Radiation Budget Satellite (ERBS) at approximately 2.1 degrees per second (deg/sec). The cause was a command sequence error that prematurely activated instead of disabled a roll thruster without roll-axis rate input. The large pitch and roll angles experienced during the tumble resulted in periodic loss of contact with the Tracking and Data Relay Satellite (TDRS) and loss of Earth contact by the horizon scanners, causing erroneous input into the magnetic control loop (MCS). Also, the rates achieved during the tumble exceed the telemetry limits for the IRU, resulting in saturated gyro data. Thus, only magnetometer and occasional Sun sensor data were available to derive attitude information during the tumble.

Analysis of the attitude sensor data from the tumble was conducted to derive continuous pointing information during the period of the tumble since both ERBE scientific instruments remained in their normal operating modes during most of the period. The analysis also included verifications of the effects of the Earth limb and the Sun on the science sensor output. The analysis and results are believed an important example and guideline for planning spacecraft support in the future.

Following a brief overview of the ERBS spacecraft, the analysis of the sensor data during the spacecraft tumble is presented. The presentation begins with a narrative description of the playback and real-time data and continues with the analysis and the results of an attempt to provide continuous ground-determined attitude solutions using playback data. A dynamic model was developed for this part of the analysis to provide continuous rate data required by the ERBS fine attitude determination system (FADS). The solutions are compared with data output from the ERBS nonscanner instrument. Finally, the application of the tools developed in this study to ERBS real-time and future mission attitude support are examined. A major portion of the work, data, and analysis presented in this paper is based on material presented more comprehensively in an October 15, 1987, memorandum prepared for the ERBS project by the FDD (Reference 1). The science sensor performance is similarly treated in more detail in a memorandum to the ERBS project written by W. Weaver, Langley Research Center (LRC) (Reference 2).

2. ERBS SPACECRAFT AND INSTRUMENT OVERVIEW

The ERBS is an Earth-pointing, momentum-biased spacecraft carrying scientific instruments to map the absorption and emission of thermal energy by the Earth. Two of the instruments, the Earth Radiation and Budget Experiment (ERBE) nonscanner and scanner, measure outgoing radiation in three broad spectral bands. The ERBE scanner is a three-channel radiometer that scans from horizon-to-horizon in a plane normal to the orbit plane. The ERBE nonscanner has two wide field-of-view (WFOV) and two medium field-of-view (MFOV) Earth-viewing channels and a Solar channel for viewing the Sun periodically. Each WFOV detector has

C. 5

a total conical FOV of about 140 deg and views the entire disk of the Earth, and a MFOV detector has a conical FOV of 90 deg. In the normal operating mode, the optical axes of the Earth-viewing detectors are aligned with the spacecraft Z-axis, and thus have their FOVs centered on the Earth at the nadir. A third science instrument is the Stratospheric Aerosol and Gas Experiment (SAGE), which views the Sun on the Earth limb to measure absorption spectra at sunrise and sunset yielding the mixing ratios of atmospheric aerosols. ERBS utilizes two analog attitude control methods, the Magnetic Control System (MCS) and the Reaction Control System (RCS) during scientific sensor operations, and orbit and attitude adjust maneuvers, respectively.

The MCS sensors and actuators are two Earth IR horizon scanners, one momentum wheel, two Scanwheels,[1] and four electromagnets. The MCS maintains the ERBS pointing to within 1.0 deg of the nominal null reference attitude on all three axes.

The RCS sensors and actuators are two redundant Inertial Reference Units (IRUs) containing three single-axis gyros for rate information to control eight 2.2 Newton hydrazine thrusters.

Attitude information for use with the science data is derived from the analog output of the onboard gyrocompass subsystem of the RCS. These data are periodically verified on the ground using the FADS, which utilizes the IRU rate, Earth infrared (IR), and Sun sensor data.

3. ATTITUDE DATA ANALYSIS AND DESCRIPTION

Three distinct phases of the yaw turn anomaly are

- The initial phase, starting at the beginning of the yaw maneuver at 15:17:08 during the action of the anomalous and constant roll thruster firing, and command execution of the still active stored yaw turn commands and occasional real-time commands

- The approximately torque-free tumble phase, which begins at 15:32:58 and continues until the initiation of the G-RATE mode to despin the spacecraft at 18:45:28 (when the thruster auto cutoff was disabled in the G-RATE mode)

- The post G-RATE mode when the spacecraft is nearly inertially despun except for a 0.06-deg rate around the +Y-axis and a switch by real-time command to the B-DOT mode at 22:08:15 universal time coordinated (UTC).

3.1 PLAYBACK DATA DESCRIPTION

The attitude sensor data used for the nominal attitude determination support are from the Sun sensors, the IR scanners, and the three-axis IRU. During the

[1]Scanwheel is a registered trademark of ITHACO Corp.

high-rate (2 deg/sec) tumble, the IRU data were saturated and of limited use except as rate polarity and rate transition time indicators. The IR scanner data were also confused with valid data occurring occasionally when the Earth scan geometry was near the geometry of the planned operation of the scanners. The data that are most illustrative of the spacecraft attitude motion during the yaw turn tumble are the data from the three-axis magnetometer and Sun sensors. The magnetometer data plotted for the duration of the playback tape are illustrated in Figure 1. The data show the beginning of the control anomaly when the thrusters were on (15:17:08 to 15:32:58) and the motion is torque driven. Next is a period of relatively constant angular momentum with no thrusting at an instantaneous spin rate of 2.1 deg/sec (15:32:58 to 18:45:28). During this period the spacecraft body is spinning around an angular momentum vector that is approximately constant in the GCI reference frame. However, the angular velocity vector moves in the body reference frame as a result of precession and nutation and in response to momentum exchange between the wheel and the body. After this high-spin period, the G-RATE mode drives the spacecraft into a near despun mode, with rates that are typically less than .1 deg/sec on all three axes. It is in this interval that the B-DOT mode is commanded, but no obvious change occurs in the magnetometer or Sun data to delineate this event.

3.1.1 MAGNETOMETER DATA

The magnetometer data in the torque-driven, torque-free, and low-rate intervals illustrated in Figure 1 show

- Oscillations at an approximate period of 2 to 3 min
- Occasional periods when the amplitude of the magnetic field oscillations goes to zero at a near-constant value on all three axes simultaneously at 16:11, 16:59, 17:48, and 18:37
- The transition in the spin rate from the nominal pre-yaw turn 1-RPO mode to the tumble and the return to the low-rate mode after the G-RATE action at 18:45:28

The four periods of low amplitude magnetic field oscillation are times when the spacecraft spin axis is closely aligned with the local magnetic field. The field at each of these times is within 10 deg of 70-deg latitude and 252-deg right ascension. The sign and magnitude of each of the three field components at these times thus gives an approximate indication of the location of the spin axis in the body reference frame and in the GCI frame. It should be noted that the Y component is always positive, the X component is zero to negative, and the Z component switches sign.

3.1.2 SUN SENSOR DATA

The Sun sensor data throughout the playback period are illustrated in Figure 2. The major feature in these data is the rapid motion of the Sun through the full range (64 deg) of the sensor field of view at approximately 2.5-min intervals. The long intervals with no Sun data correspond to spacecraft night. The period from sunrise at 16:37 to the first Sun data at 16:51 is an interval where the geometry of the spin vector keeps the Sun out of the sensor field of view for

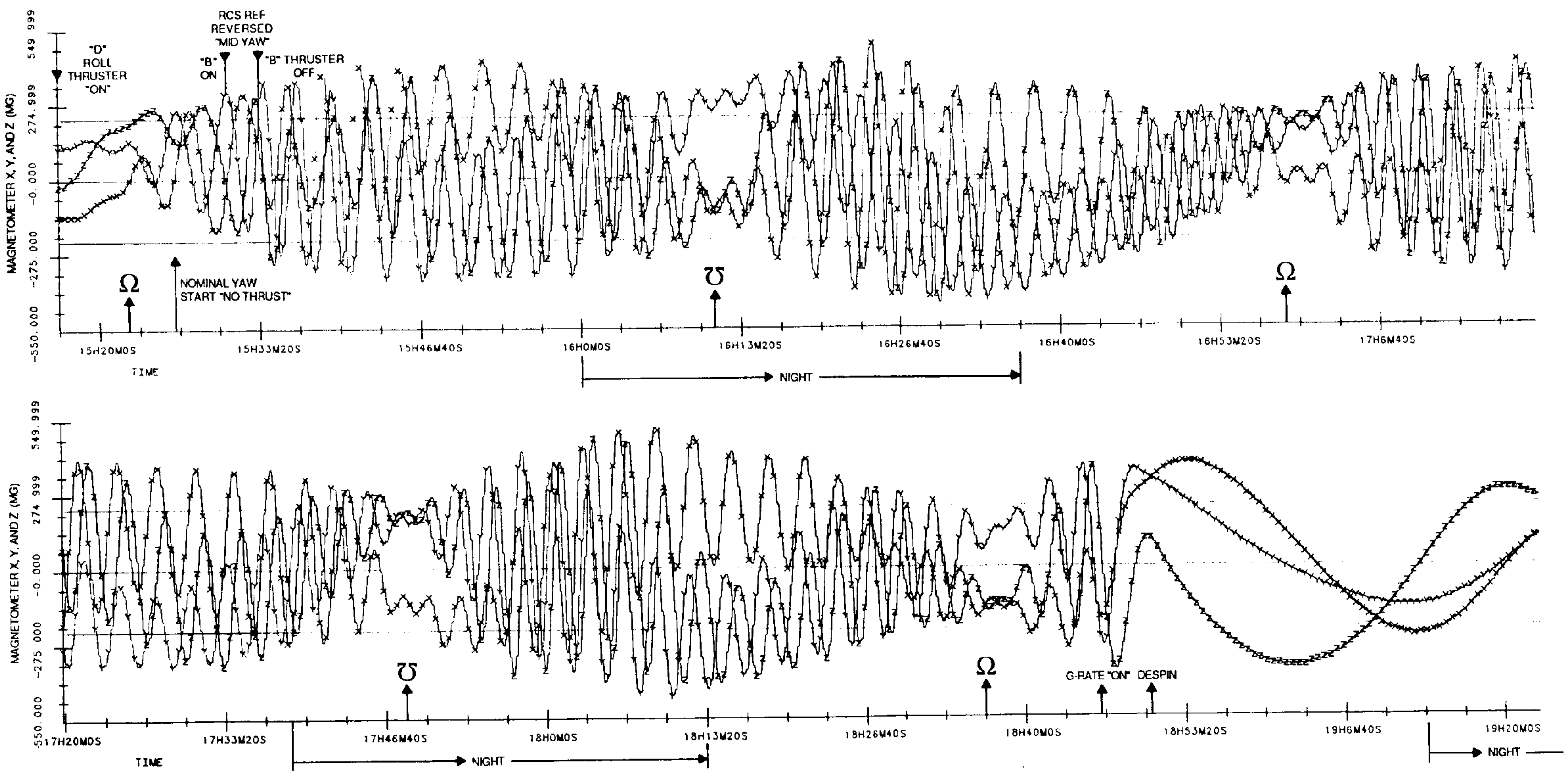

Figure 1. Magnetometer Playback Data During the ERBS Yaw Turn Tumble (1 of 2)

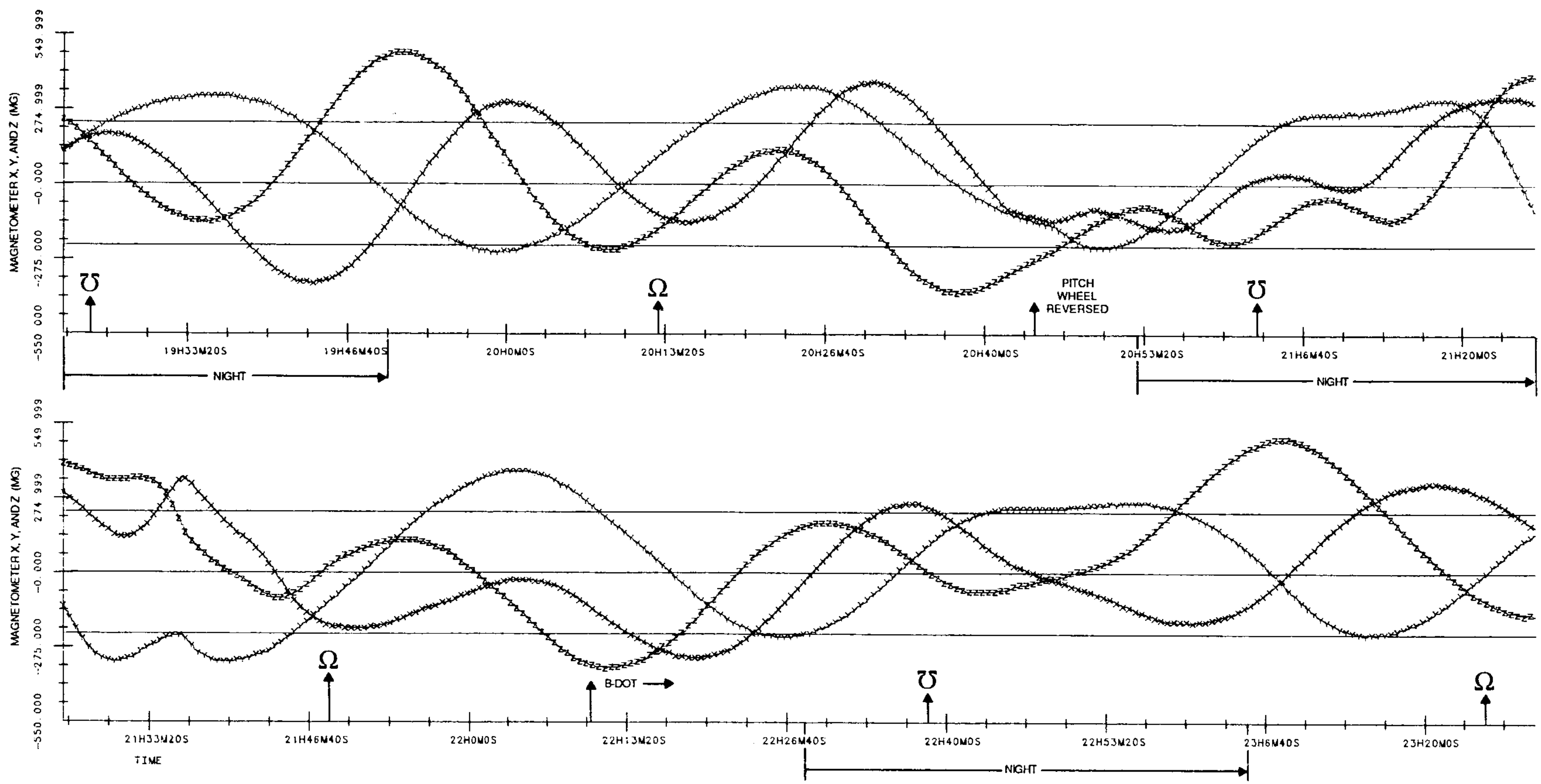

Figure 1. Magnetometer Playback Data During the ERBS Yaw Turn Tumble (2 of 2)

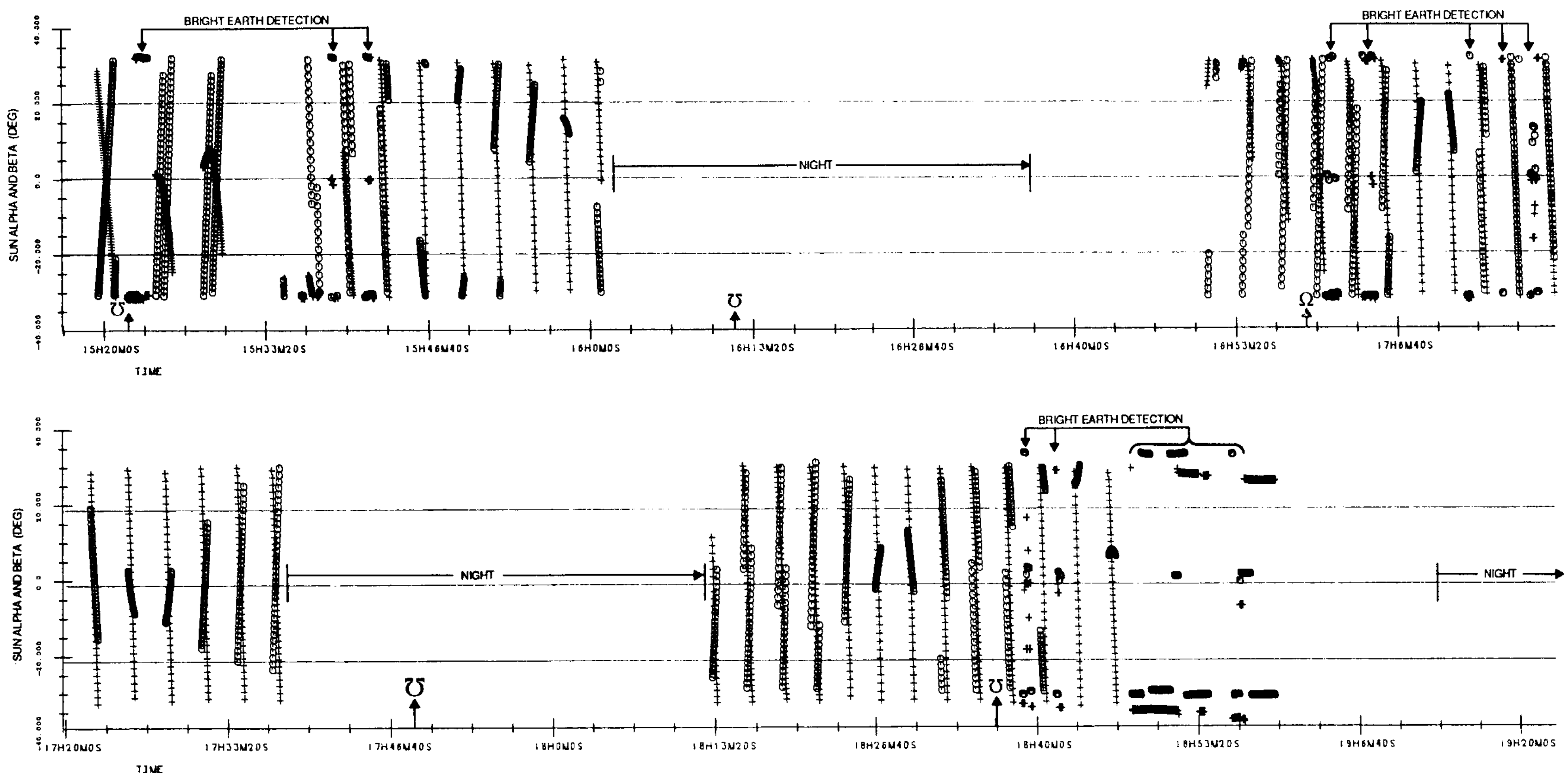

Figure 2. Sun Sensor Playback Data (15:16 through 19:20 UTC) Alpha Angles (O), Beta Angles (+)

three to four spin cycles. The corner of sensor 2 begins to encounter Sun at 16:51. Another feature in the Sun data is the stimulation of the fine reticle and coarse Gray code by reflected light off the Earth. These data can be seen at 17:17 and 18:38. Other intervals of Earth light stimulation of the Sun sensor are primarily fine reticle events with the Gray code at midrange or at the all ones or all zeros limits; these are the data at 17:01 and 15:39.

In the low-spin-rate mode, after the G-RATE mode despin, the spacecraft is aligned with the -Y-axis close to the Sun (<20 deg). In this orientation, the Sun sensor views the Earth during the orbit day and space during orbit night; also for this orientation the solar array normal is near-orthogonal to the Sun vector. The fine and coarse reticle, Earth-stimulated Sun sensor data occur at orbital positions that are about 10 min (40 deg) from spacecraft noon.

3.1.3 INFRARED SCANNER DATA

The IR scanner data are illustrated in the upper half of Figure 3. To be useful for the attitude processor, in the high-rate tumble mode, the data would require extensive filtering beyond what is available in the ERBS ADS Data Adjuster Subsystem. For this reason the data were not used in this analysis except for an attempt to select only data that could be verified as originating from near nominal Earth viewing geometry during the spacecraft nighttime period. The results from this were deemed unacceptable.

3.1.4 GYRO DATA

The gyro-rate data, illustrated in the lower half of Figure 3, are presented to illustrate the characteristics of these data during the high-rate tumble. For the nominal attitude processing, the design of the ERBS ADS could not accommodate these data. The information contained is an accurate measure of the polarity and duration of polarity for rates on the body axes; also apparent is a record of the time at which the rates are switching sign. For this analysis, these data were used to verify the dynamic modeling (described later in Section 3) of the first 5 min of the high-torque interval, and for dynamic state initialization. Approximate agreement was obtained for the polarity switch in the X-gyro rate at 15:24.

3.2 REAL-TIME DATA DESCRIPTION

The real-time data received during the ERBS yaw turn anomaly requires attention in this review because it is an example of the type of data that will be relied on in future spacecraft emergency recovery support. Also, for future preparedness, it is a useful exercise for spacecraft attitude control analysts to review these data to translate the experience to other missions. During the real-time monitoring of the yaw turn maneuver, the data that most vividly illustrated the onset of the problem were the Sun sensor data. These data, illustrated in Figure 4, are from two real-time passes. The 15:16 to 15:30 pass is from TDRS; the 17:02 to 17:13 is from Merritt Island (MIL). Sun data were not expected at the time of the maneuver. The occurrence of Sun sensor data near 15:18 was, therefore, a strong indicator of the problem. The characteristics of the real-time data reveal the complexities of real-time support

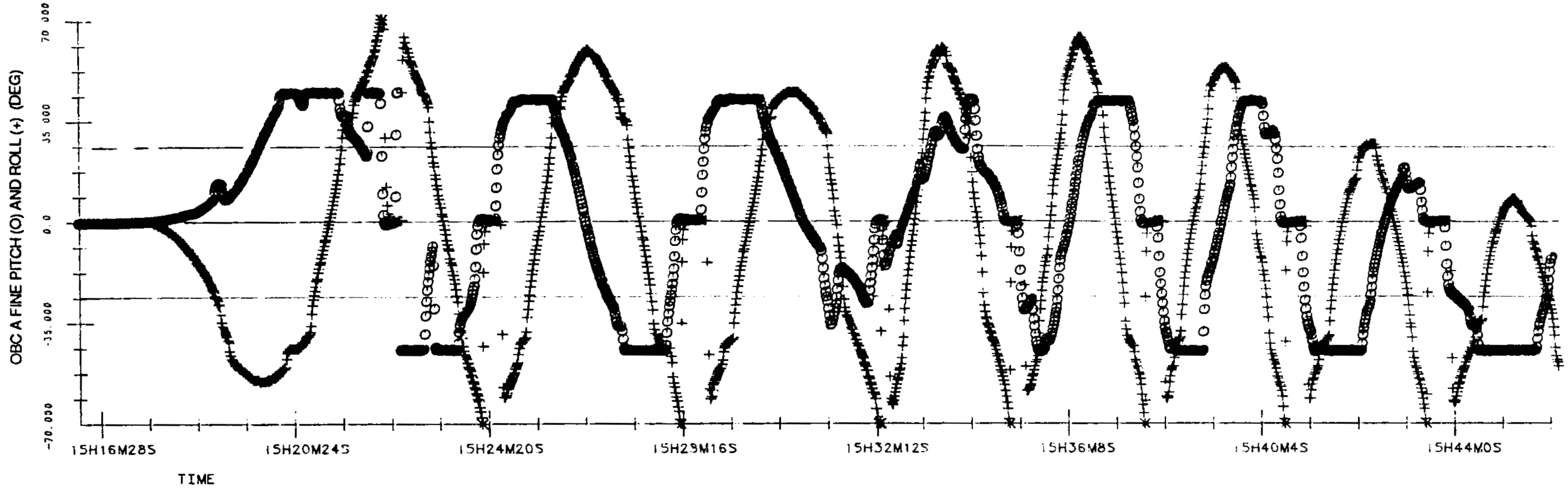

Figure 3(a). IR Scanner

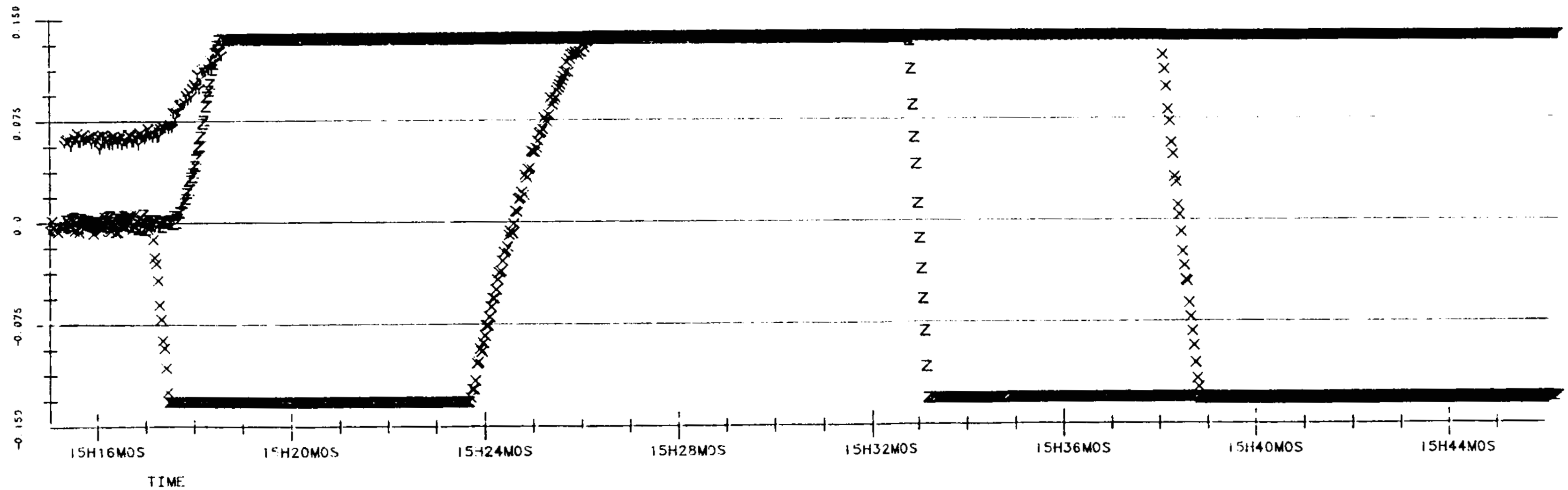

Figure 3(b). IRU Rate

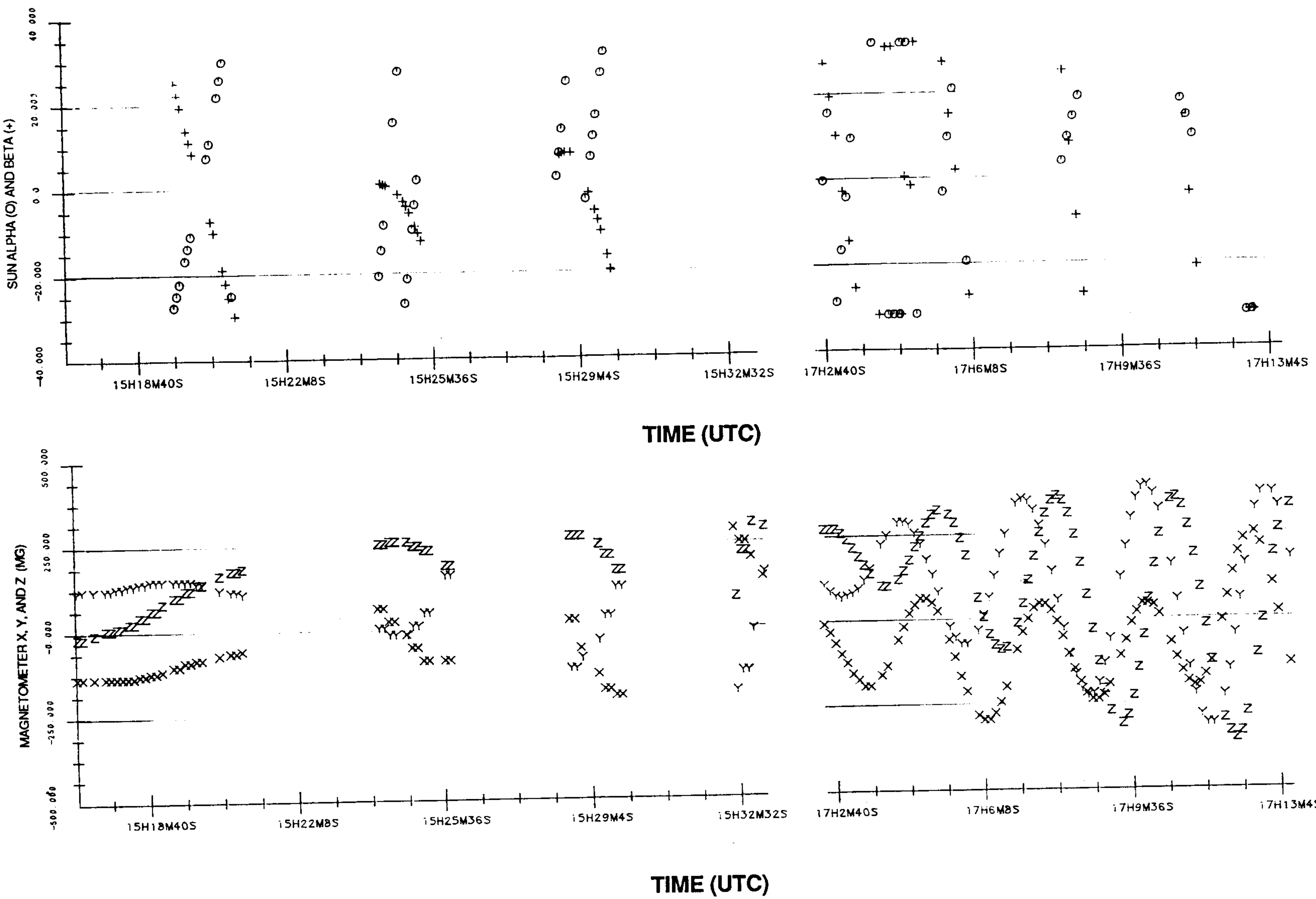

Figure 4. Real-Time Data From the First Two Passes (TDRS and Merrit Island) Sun Sensor α and β Angles (Upper) Magnetometer x, y, z (Milligauss) (Lower)

with these data. The first feature is that the telemetry during the TDRS contact data are periodic at approximately the tumble period, as expected from a sensor with a wide field of view periodically scanning the Sun at the spacecraft spin rate. However, the geometry of the MIL pass and omni RF beam does not cause obvious strobing. Not immediately obvious, however, was the fact that the TDRS contact data were being strobed by the telemetry downlink interruptions caused by the rotation of the omni antenna hemispherical radio frequency (RF) beam. Had the control center support been performed for this maneuver or similar command load events using a TDRSS high-gain antenna, the availability of the data and command RF link following the control error would have been severely limited. The strobing of the data by the RF was not noticed immediately in the Flight Dynamics Facility (FDF). It became apparent when an attempt to plot the Sun trace in the sensor field of view showed that it occasionally started or ended in the middle of the field of view on consecutive spin rotations. The telemetry strobing is more obvious in the magnetometer and IRU data from the TDRSS pass illustrated in the lower portion of Figure 4 and Figure 5, respectively. For a real-time contact, these data should be contiguous throughout. The IR scanner data are illustrated for completeness in the upper half of Figure 5.

4. ATTITUDE DETERMINATION WITH DYNAMICS

The FDF ERBS Attitude Ground Support System (AGSS) includes two attitude estimation methods: the quaternion estimator (QUEST) for the coarse attitude determination system (CADS) and the batch least-squares routine for the FADS. The QUEST algorithm requires at least two sensor observation vectors per frame to derive the optimal attitude quaternion. The batch least-squares algorithm uses the IRU as a motion model to propagate the attitude from a solution at an epoch. Sun and IR horizon data are used to determine the epoch attitude and the gyro biases.

The data from the anomaly cannot be used directly in either technique for continuous attitude determination. QUEST cannot provide continuous solutions due to the lack of two valid observation vectors when Sun data are not present. The FADS could not be used because it requires contiguous, unsaturated IRU telemetry data. Therefore, a dynamic model was developed to fill in the intervals of saturated IRU telemetry. Previous attempts at this procedure had shown substantial errors for long periods of modeling (Reference 3). For the tumble, however, only short segments of modeling are required due to the presence of Sun data every 2 min.

4.1 THE DYNAMIC MODEL

The dynamic model uses Euler equations of motion to determine the spacecraft body rates in the saturated intervals. This is followed by an application of the FADS, which fills the 3-min periods between Sun data for up to 6 minutes of propagation. The differential corrector was applied to the model to determine a constant torque bias for each axis. The objective of the corrector was to achieve body rates within .01 deg/sec of the known rates during Sun periods.

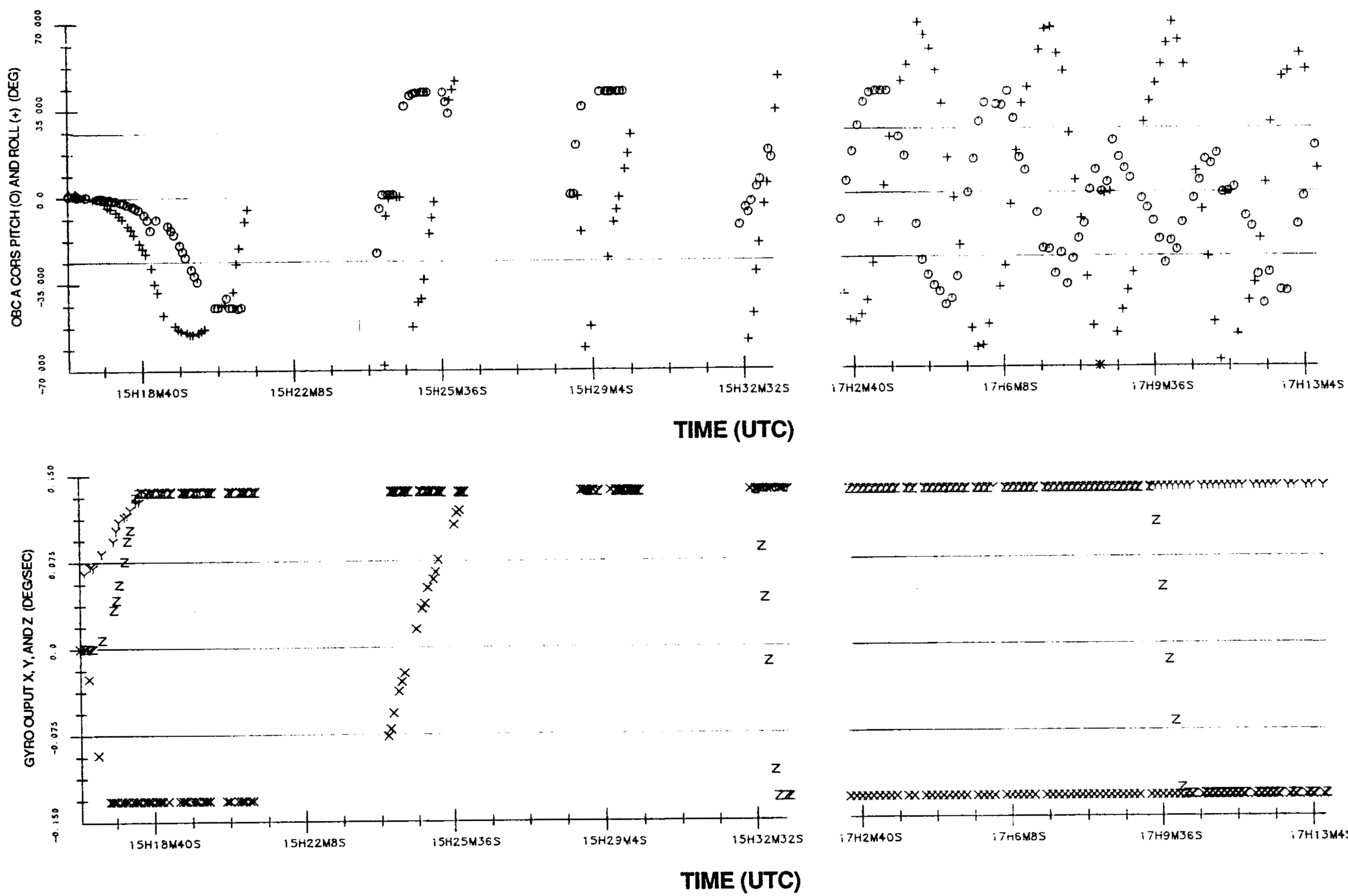

Figure 5. Real-Time Data From TDRSS (Left) and MIL (Right); IR Scanner Pitch and Roll (Upper); IRU x, y, and z Body Rates (Lower)

The dynamic motion model from the Euler equations of motion is

$$I\frac{d\tilde{\omega}}{dt} = \tilde{N} - \frac{d\tilde{h}}{dt} - \tilde{\omega}x(I\tilde{\omega} + \tilde{h})$$

where I = 3 x 3 moment of inertia matrix
$\tilde{\omega}$ = body angular rate vector
$\tilde{h}$ = sum total angular momentum of the wheels in the body frame
$\tilde{N}$ = external torque vector (thruster and environmental)

The equations of motion are integrated numerically using the fourth order Runge-Kutta method. The quantities $\tilde{h}$ and $\frac{d\tilde{h}}{dt}$ are determined from the wheel speeds in the playback data, where $\frac{d\tilde{h}}{dt}$ is taken to be constant between wheel speed samples.

The Gauss-Newton least-squares estimator is employed to estimate the initial state vector from the intervals of valid data. The state vector is composed of the following parameters:

- Initial spacecraft body angular rates
- Scale factors for each resultant thruster torque
- External torque bias

The batch least-squares method requires the comparison of the observation data to a sensor data model which is based on the state vector which evolves according to the dynamic motion model. The observations used are valid IRU rate data during the occasional nonsaturated transition intervals and Sun sensor data. A Sun sensor data model is derived by letting the model vector equal the observed at the first occurrence of a valid observation. At time Δt (= 1 sec) the Sun vector model is calculated from

$$\tilde{S}_{mt2} = \frac{\tilde{S}_{mt1} + \tilde{S}_{mt1} \times \tilde{\omega}_B \Delta t}{|\tilde{S}_{mt1} + \tilde{S}_{mt1} \times \tilde{\omega}_B \Delta t|}$$

The gyro rate ($\tilde{w}_B$) is taken directly from the integrated equations of motion.

The state vector is determined iteratively using

$$\tilde{x}^0_{K+1} = \tilde{x}^0_K + \left[S_0 + G_K^T W G_k\right]^{-1} \left[G_K^T W(\tilde{y}-\tilde{g}_k) + S_0\left(x^0_A - \tilde{x}^0_K\right)\right]$$

which is a result of minimizing the loss function, (J), where

$$J = \frac{1}{2}(y - g)^T W(\tilde{y} - \tilde{g}) + \frac{1}{2}\left(\tilde{X}^0 - \tilde{X}^0_A\right)^T S_0 \left(\tilde{X}^0 - \tilde{X}^0_A\right)$$

and $\tilde{x}^0_K$ = Kth estimate of the state vector at the epoch

x^0_A = a priori estimate of the state vector at the epoch

S_0 = diagonal state weight matrix

W = diagonal observation weight matrix

G_k = matrix of model partial derivative of the form $\frac{\partial \tilde{y}}{\partial \tilde{x}^0_K}$

$\tilde{y}$ = observation vector

$\tilde{g}_K$ = sensor observation model vector

To replace the saturated gyro data, the dynamic iteration model is employed in the following manner. The playback data are processed in the AGSS, flagging all saturated gyro and invalid Sun data. These data are written to a data file that can be accessed by other software.

The dynamic model uses these data for a user-specified time segment. This time segment is usually the interval from the middle of one Sun occurrence to the middle of the next. The a priori estimate for the angular rates is determined from the final rates of the previous batch. When the previous batch is not available, the initial rates are determined by processing a small segment of time through the dynamic model. By weighting the a priori estimate of the torque biases, the dynamic model will converge on an accurate estimate of the body rates. These rates are then used for the a priori estimate of the entire time interval.

The body rates resulting from the solved-for state vector are used to replace the IRU rates in the data file read by the FADS. The FADS is then used to determine continuous attitude solutions over the high-spin rate interval by propagating from an epoch attitude and rate bias using attitude variation from the dynamically interpolated rates.

4.2 ATTITUDE RESULTS

An example of the pitch, roll, and yaw angle results from the dynamic interpolation is shown in Figure 6. Since the dynamic motion model used was not accurate enough to span time gaps exceeding 6 min, this technique was not applied to the night periods.

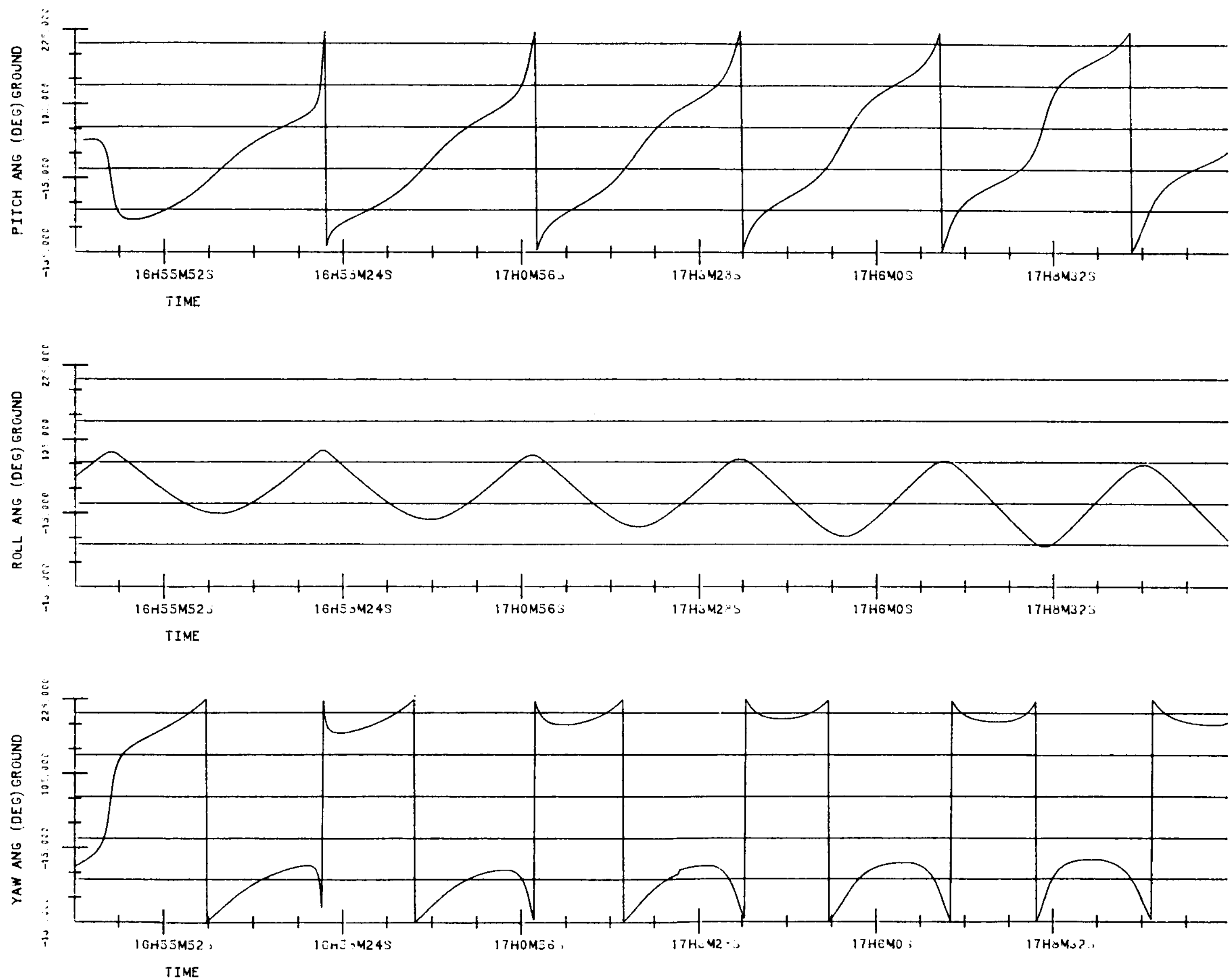

Figure 6. The Pitch, Roll, and Yaw Attitude From Dynamic Interpolation of the Sun Sensor Data

For the period after the tumble was halted, the IRU data returned to nominal, and the attitude could be calculated directly using FADS with magnetometer data.

The attitude solutions obtained from the dynamic interpolation of the IRU data during the high-rate tumble and from the FADS for the despun mode were used to plot the motion of the Sun on the unit sphere of the body reference frame (BCS). Figure 7 covers two intervals of high-spin rate and low-spin rate data. The low-rate data are from the time immediately following the command to the G-RATE mode when the spacecraft is despun using thrusters. The two spheres on each page of the figure show the BCS frame oriented with the +Z-axis downward as in the ERBS configuration of nominal flight. The +Y-axis side of the BCS is the left-hand sphere with the Sun sensor field of view inscribed on the sphere to allow correlation of these data with the Sun sensor data displayed in Figure 7. The left-hand sphere is the -Y-axis side of the BCS viewed from slightly below the X-Y plane. The Sun traces on the sphere are labeled with numbered tick marks at 30-sec intervals for the data corresponding to the high-spin-rate mode. The ERBE science sensor 45-deg and 70-deg fields of view are also delineated as cones around the +Z-axis. The solar array field of view, which is depicted here as a 2π steradian field 11 deg off the -Z-axis, is also illustrated to show when the Sun was shining on the array. The sphere-plot representations of the despun Sun traces, such as those in Figure 7(b) for the whole recorded interval, indicate that for all but 50 min of the daytime periods between 18:43 UTC and 23:00 UTC, the Sun was off the solar array.

5. COMPARISON OF CALCULATED SPACECRAFT POINTING DATA WITH ERBE NONSCANNER INSTRUMENT DATA

Both ERBE instruments remained in their normal operational modes from the beginning of the yaw anomaly on July 2 until after the primary rotation of the spacecraft was stopped. The nonscanner detectors were pointed along the spacecraft positive Z-axis, and the scanner detectors were scanning in a plane that is normal to the spacecraft X-axis. Data indicate that the fields of view of both instruments were exposed to direct solar radiation. The scanner detectors respond erratically when exposed to the strong solar radiation, making it difficult to accurately resolve when the exposure begins and ends. Thus, only nonscanner instrument data acquired during spacecraft rotation are described.

Figure 8 shows the raw output (one measurement every 16 sec) of the wide field of view total radiation detector for the period on July 2, starting before the yaw maneuver began and ending a few minutes after the rapid motion of the spacecraft was stopped. The period of the data begins with the detectors viewing the Earth in full darkness. The raw output of the detector is a maximum for zero input radiation and decreases with increased input radiation. The first isolated spike seen in the detector data of Figure 8 indicates when the detector viewed the Sun at the spacecraft horizon as the spacecraft passed from darkness into sunlight. This spike is normal in the nominal mission mode, occurring twice each orbit. Comparing this Sun spike to data obtained during

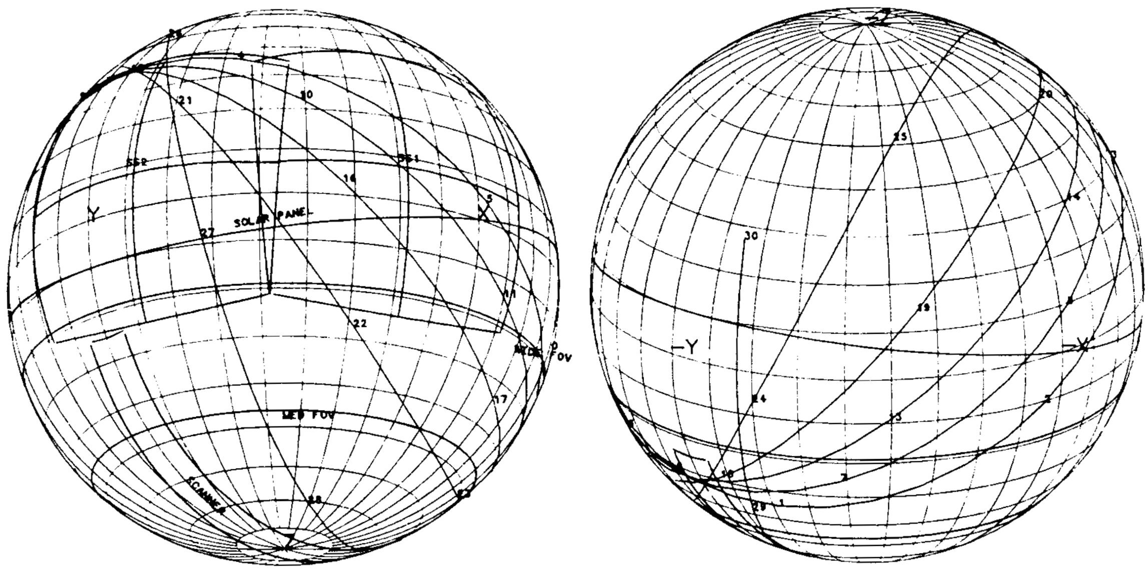

Figure 7(a). Sun Traces in the Body Frame From 1655 to 1710 (Tick Marks Every 30 sec)

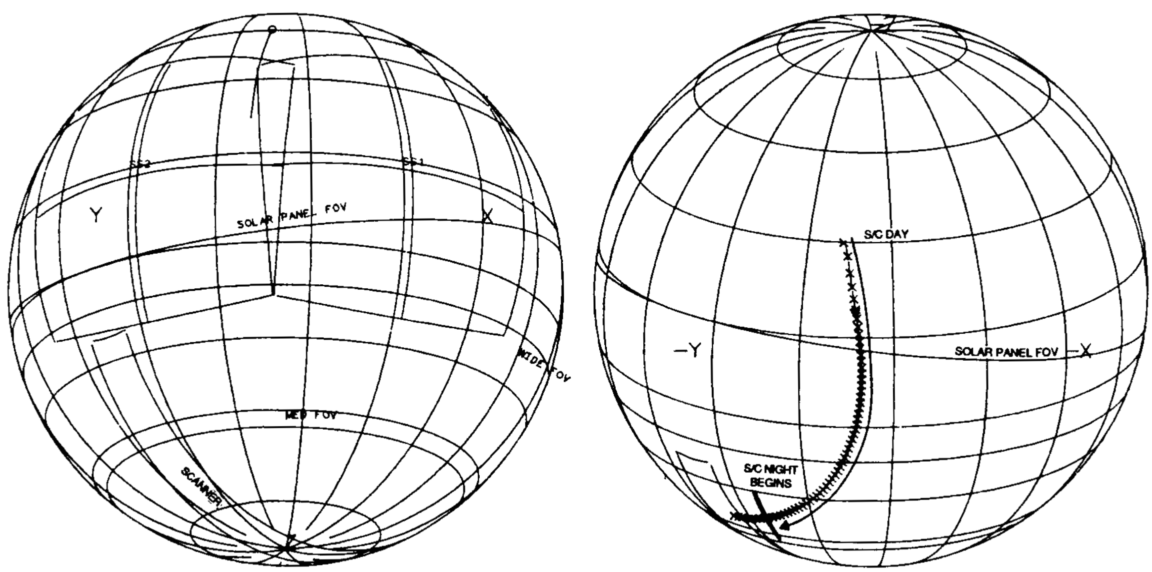

Figure 7(b). Sun Traces in Body Frame From 870702.184301 to 870702.192101 (0 = Start Time, X at Every 30 sec)

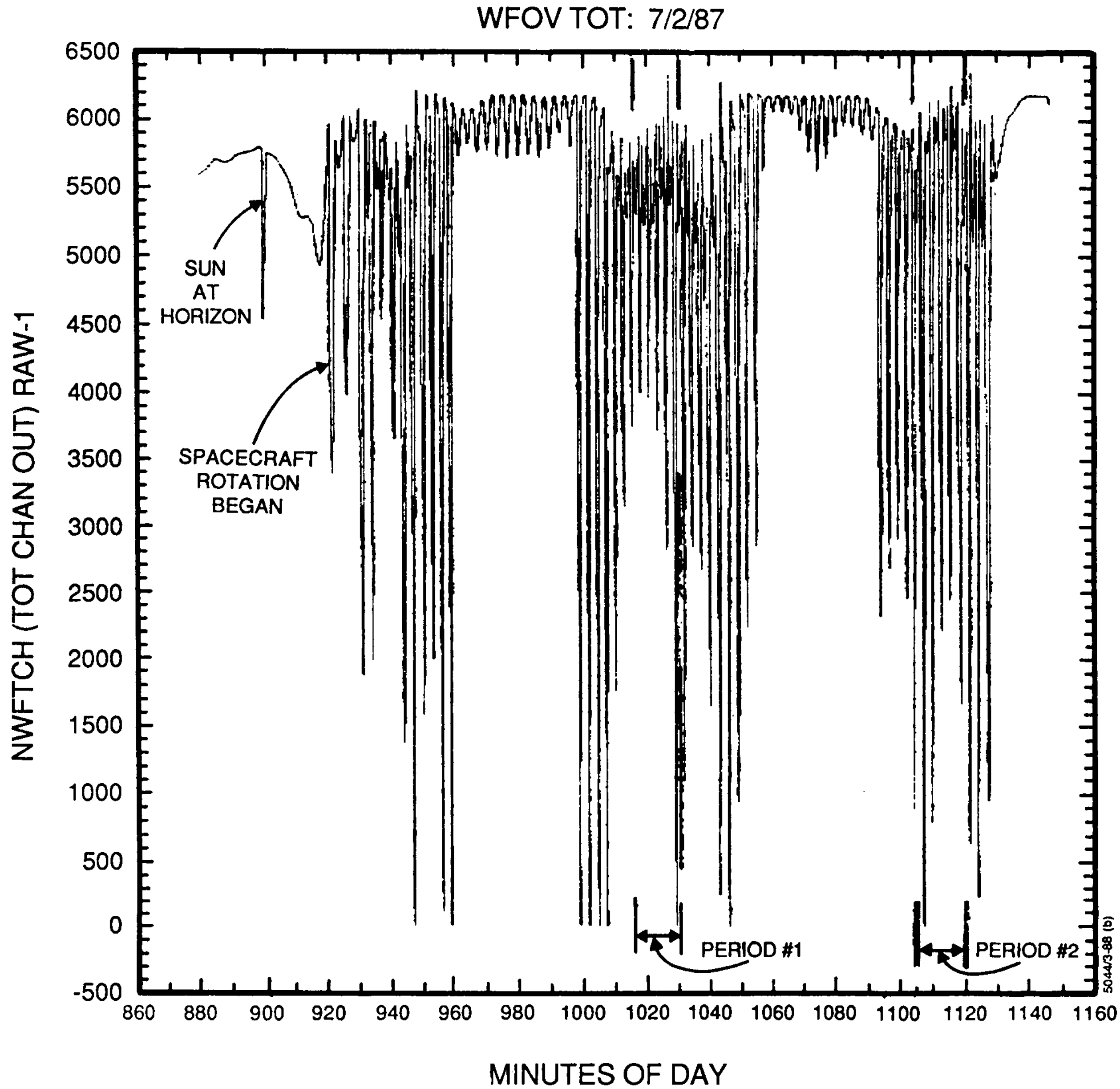

Figure 8. Raw Radiance Signal From the Wide Field of View ERBE Nonscanner from 15:00 UTC to 19:00 UTC

the period of spacecraft rotation, it appears that the wide field of view detectors sensed some solar input about every 3 min during the sunlight portions of the three orbits that the spacecraft was rotating.

Raw radiometric data from the wide and medium fields of view total detectors for the two 15-min periods identified in Figure 8 are presented on enlarged time scales in Figures 9 and 10 along with corresponding plots from the calculations of the angular separation of the detector fields of view from the Earth nadir and Sun vectors using attitude results based upon the dynamic interpolation.

From the attitude angles, the angles from the edges of the field of view of both a wide angle (70 deg) and medium angle (45 deg) nonscanner to the nadir vector and the Sun vector were calculated. These values correspond to the data in the upper sphere plot of Figure 7. The solid line indicates the wide angle nonscanner limits, and the dashed line indicates medium angle nonscanner field of view limits. From the graphs, the time when either experiment viewed the Sun or the Earth can be determined. To view the Sun, the edge of the field of view must include the Sun line, which is the zero angle in the upper graph. To view the Earth, the field of view edge must include the Earth edges, which are the lines of constant value ±70 deg in the lower graph.

The calculated field of view envelope data indicate that the wide field of view detector received solar radiation during every spacecraft rotation cycle from 16:55 to 17:10 and that the medium field of view detector sensed the Sun only during the last two cycles. These calculations are verified by the corresponding detector output data of Figure 9. The increasing Solar exposure predicted for the wide field-of-view detector can also be seen clearly during the last two rotation cycles in Figure 9. The Earth-view predictions and comparisons with detector output data are not as interesting. However, the calculations, which predict Earth views every cycle for both detectors, are confirmed by the raw radiometric data of Figure 9. Two features of the calculated field of view envelope data for the period from 18:25 to 18:40 (Figure 10) are confirmed by the ERBE instrument radiometric data for that period. Solar exposure was greatest during the second rotation cycle (about 18:27), and Earth radiation exposure was greatest during the last cycle (about 18:40).

6. CONCLUSION

A description of the characteristics of the ERBS yaw turn attitude control anomaly, which occurred during an in-flight test of the X-gyro disabled yaw inversion maneuver plan, has been presented. Processed attitude sensor data from playback data augmented by a dynamics model has provided a complete description of the attitude history throughout the sunlit period of the control anomaly covered by the playback data. Verification of the method applying the dynamic model to interpolate the IRU data was performed by direct comparison of calculated science sensor boresight to Sun and Earth angles with raw IR intensity data from the ERBE nonscanner. Examples of the attitude sensor data received in the real-time telemetry data illustrated the complication that

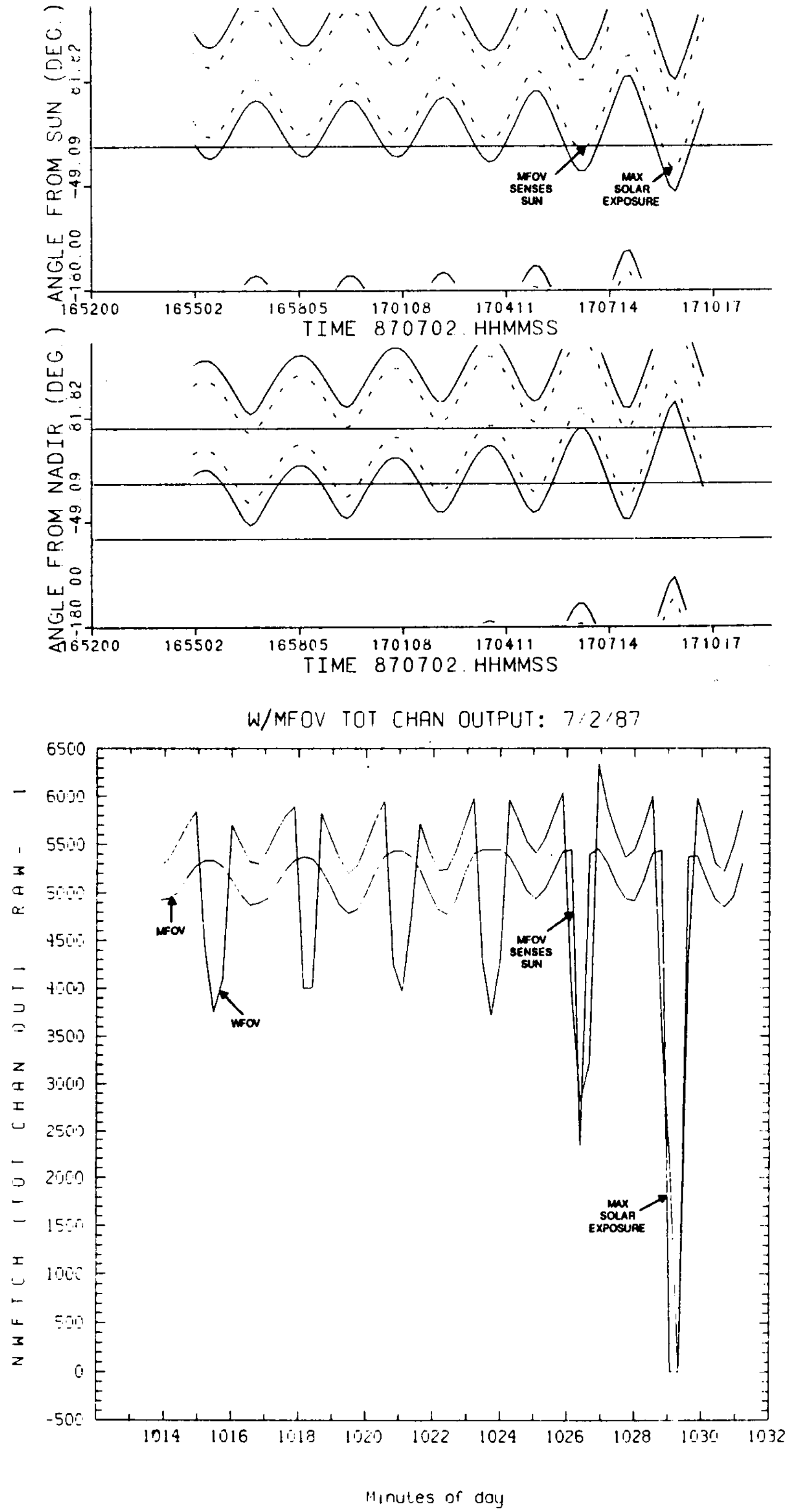

Figure 9. A Comparison of the ERBE Nonscanner Sun and Nadir Angle Computations (Upper) With the ERBE Nonscanner Raw Radiometric Output From 16:55 UTC and 17:10 UTC

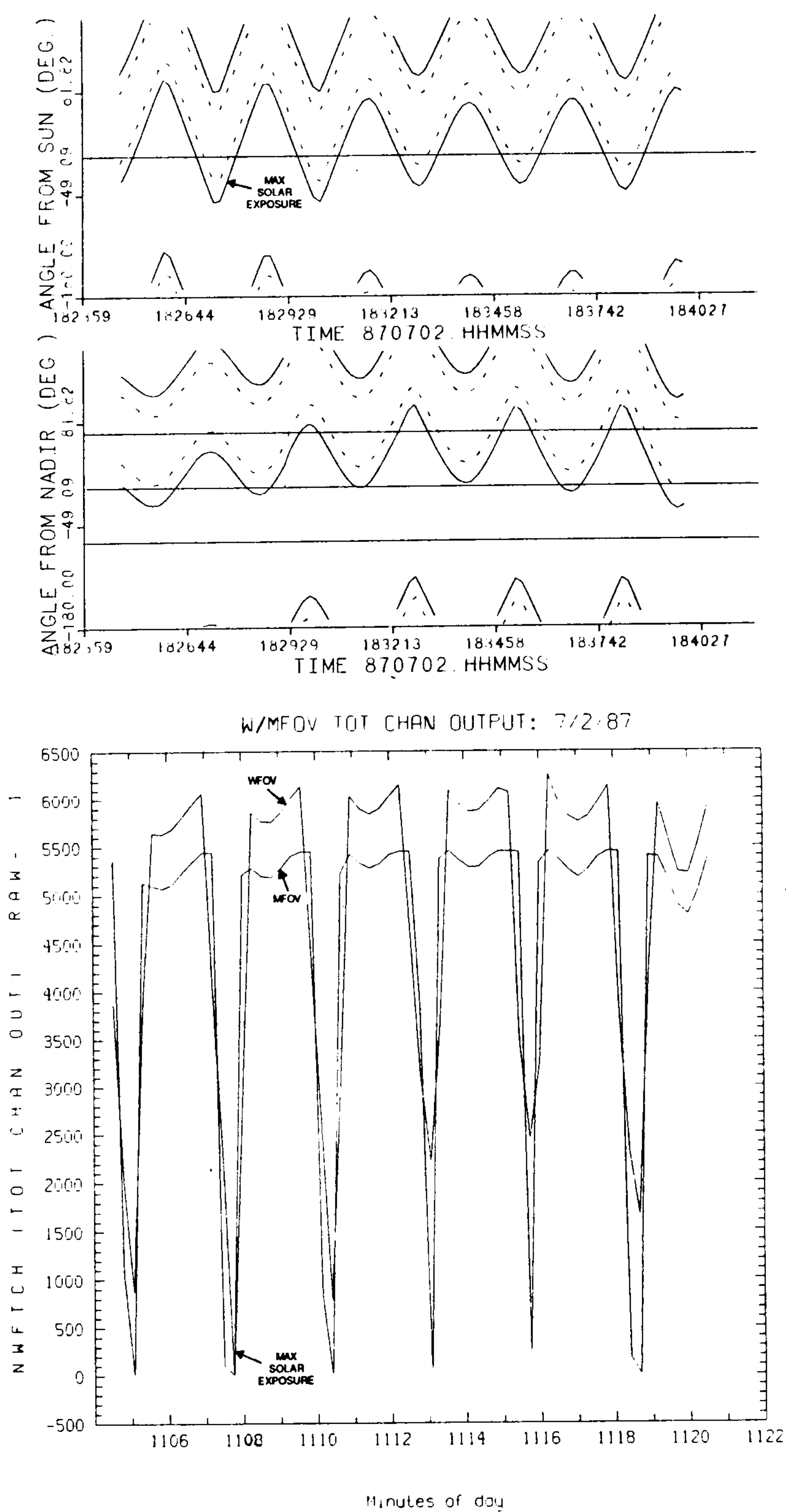

Figure 10. A Comparison of the ERBS Nonscanner Sun and Nadir Angle Computation With the Raw Radiometric Output From 18:24 UTC to 18:40 UTC

telemetry strobing imposes on real time commanding and attitude telemetry interpretation. The playback data revealed the phenomenon of stimulation of the fine Sun sensor by the Earth albedo at orbital locations approximately 40 deg on either side of the subsolar point. The analysis of the July 2, 1987, ERBS yaw turn anomaly has provided an opportunity to assess the software and procedures requirements for support of spacecraft emergencies in the FDF.

In retrospect, the following observations can be made about the experience pertaining to the contingency support procedures and software. The point of view is taken relative to the real-time event, and, therefore, it is imperative not to assume that data quality and diagnostic resources are near those provided by the playback data analyzed and presented in this work.

1. Real-time telemetry was useful for the initial problem diagnostics, including the tumble state and a rough estimate of the spacecraft body rate. These data also provided the Sun sensor data for the early hand-drawn versions of the Sun traces in the BCS frame field-of-view plots. These plots were then instrumental in demonstrating the telemetry strobing and providing crude estimates of the evolution of the spin axis in the BCS frame. Beyond this, the real-time attitude telemetry was of limited use with the software and procedures that were in place at the time.

2. Later, after the entry into the despun mode and even later during the activation of the B-DOT control mode, occurrences of unflagged (Sun presence "on") Sun sensor data led to incorrect conclusions about the despun orientation, which if acted upon could have further complicated the situation. These were subsequently (days later) determined to have been caused by the bright Earth light.

3. Valid solutions to the attitude in the periods of high-spin rate were possible using the ERBS CADS; however, the attitude representation of pitch, roll, and yaw was not suited for the spinning and nutating condition. This suggests that the availability of alternative representation, such as the spin-axis right ascension and declination, BCS spin unit vector, and angular momentum vector representations, may have contributed to a more rapid resolution of the detailed attitude and spacecraft spin state from the limited real-time data.

4. Reliable spacecraft dynamics simulation in conjunction with attitude determination using Sun sensor and magnetometer data could contribute significantly to the real-time attitude estimation process in the contingency mode.

5. An attitude algorithm relying only on the magnetometer data with initialization during periods of valid Sun sensor and gyro data or during those special periods of coalignment of the spin axis and the geomagnetic field, in addition to optional choices for the attitude state representation would probably have been the most useful tool. The usefulness of such a software tool would have been directly proportional to the graphics capabilities and the ability to quickly generate hardcopy versions of attitude results in some of the optional representations presented in this work.

REFERENCES

1. CSC Memorandum Analysis of the ERBS Attitude Motion During the July 2, 1987, Control Anomaly, J. A. Kronenwetter and M. C. Phenneger (CSC), October 1987

2. Langley Research Center Memorandum, Analysis of the ERBE Instrument Data Around Time of ERBS Yaw Maneuver Anomaly on July 2, 1987, W. Weaver (NASA/LRC) and M. G. Payton, (STX Corporation), September 4, 1987

3. E. J. Lefferts (GSFC) and F. L. Markley (CSC), Dynamic Modeling for Attitude Determination 76-1910 AIAA Guidance and Control Conference, San Diego, California, August 16-18, 1976